

The “Hidden” Phase Diagram of Water + 3-Methylpyridine at Large Absolute Negative Pressures

Zoran P. Visak, Luís P. N. Rebelo,* and Jerzy Szydlowski†

*Instituto de Tecnologia Química e Biológica, ITQB 2, Universidade Nova de Lisboa,
Av. da Republica, Apartado 127, 2780-901 Oeiras, Portugal*

Received: October 28, 2002; In Final Form: January 29, 2003

Liquid–liquid (L–L) phase splitting in mixtures of water (H/D) + 3-methylpyridine (3-MP) at the limit of pure H₂O as solvent and under high tension are reported for the first time. The phase diagram is thus encountered at large absolute negative pressure regimes. To the best of the authors’ knowledge, these studies constitute the first to report phase transitions in nonpolymeric fluid mixtures at negative pressures, and the values of tension achieved (≈ -350 bar) constitute a record for macroscopically sized samples. The overall behavior of mixtures of water (H/D) + 3-MP is successfully interpreted by using a simple g^E -model. It is clearly shown that there is an intimate relation between pressures and the isotopic content of the solvent, and, thus, the latter can act as a thermodynamic variable. At critical concentrations, while mixtures of D₂O + 3-MP always present phase separation irrespective of the applied pressure, when the solvent is pure H₂O a miscibility window with the size of 1600 bar emerges. This phenomenon corresponds to an impressive pressure shift of several hundred atmospheres upon (H/D) solvent isotopic substitution. When this effect is projected onto the temperature–solvent isotopic content at atmospheric pressure, a 70 K immiscibility loop is encountered when D₂O acts as the solvent, while total miscibility occurs for concentrations of D₂O (in D₂O + H₂O) lower than 17 wt %. It is shown that an entropic effect originated at the relatively large difference in molar volumes between water and 3-MP is responsible for the location of the L–L phase diagram in the low-concentration region of 3-MP. It is again another (but subtle) entropic effect that provokes the above-mentioned abnormally large shift in the phase diagram upon isotopic substitution.

1. Introduction

While it is well-known that, at atmospheric pressure, mixtures of D₂O + 3-MP exhibit a closed-loop type of (T, x) phase diagram¹ and that H₂O + 3-MP mixtures do not phase separate at any temperature and/or proportions of the components,^{1–3} the presence of a phase diagram for the latter system at absolute negative pressures has been speculated^{2–4} but has never been experimentally proven. In contrast, the high (positive) pressure immiscibility when water is used at several distinct H/D ratios is already well mapped⁵ up to about 300 MPa. In summary, while the (D₂O + 3-MP) system exhibits a “tube”-like type of (T, p, x) phase diagram, (H₂O + 3-MP) only presents a high-pressure immiscibility dome (if one limits pressure to its positive side); see Figure 1. The phase diagram of interest should thus be a 4-D plot, for instance, $T-p-x_{3\text{-MP}}-W_{\text{D}_2\text{O}}$, where $x_{3\text{-MP}}$ is the mole fraction of 3-MP in solution and $W_{\text{D}_2\text{O}}$ is the weight percent (wt %) of D₂O in the solvent (H₂O + D₂O). Figure 1 sketches two possible 3-D representations. At atmospheric pressure (nominal $p = 0$) and as the deuterium content increases, one finds that at ~ 17 wt % of D₂O in (D₂O + H₂O) a “single dot” in the $T-x$ plane of the phase diagram appears at $x \sim 0.08$ (~ 30 wt %) of 3-MP in (3-MP + water (H/D)) and $T \sim 350$ K. As one adds more D₂O, miscibility worsens, and a closed-loop diagram emerges. At the limit of pure D₂O as solvent, the difference between T_{UCST} and T_{LCST} amounts to

more than 70 K. If pressure is now moderately applied, the closed-loop shrinks. Thus, deuteration and (moderate) pressurization have opposite effects on the phase equilibrium behavior, and, therefore, the deuterium content has been many times used as a thermodynamic variable^{6–8} to assist the study of critical phenomena in this type of mixtures.

The richness and unique properties of the phase diagram of the (water + 3-MP) system have made it an extremely appealing candidate for the study of the divergences of response functions to criticality. Several double critical points (DCP) can be found. Because the system presents both low- and high-pressure immiscibility (upper critical solution pressure (UCSP) and lower critical solution pressure (LCSP), respectively) at both low- and high-temperatures (lower critical solution temperature (LCST) and upper critical solution temperature (UCST), respectively) and they merge under well-defined p, T conditions, these mixtures have pressure-double critical points (p-DCP)⁹—at the merge of the UCSP and LCSP—as well as temperature-double critical points (T-DCP)⁹—at the merge of the LCST and UCST. It is thus a suitable system to study anomalies in both the exponents and amplitudes of the divergences of several functions as they approach criticality (the so-called “doubling” effects). These two kinds of double critical points are also commonly called hypercritical points due to the intrinsic property that the derivative of the critical line is infinite, $(dp/dT)_c = \infty$ or $(dT/dp)_c = \infty$, respectively (see Figure 2). Their close vicinity in the T, p, x space is named the hypercritical region. Also, fundamental thermodynamic laws dictate that^{9,10} while at

* Corresponding author. E-mail: luis.rebelo@itqb.unl.pt.

† Permanent address: Chemistry Department, Warsaw University, Zwirki i Wigury 101, 02-089 Warsaw, Poland.

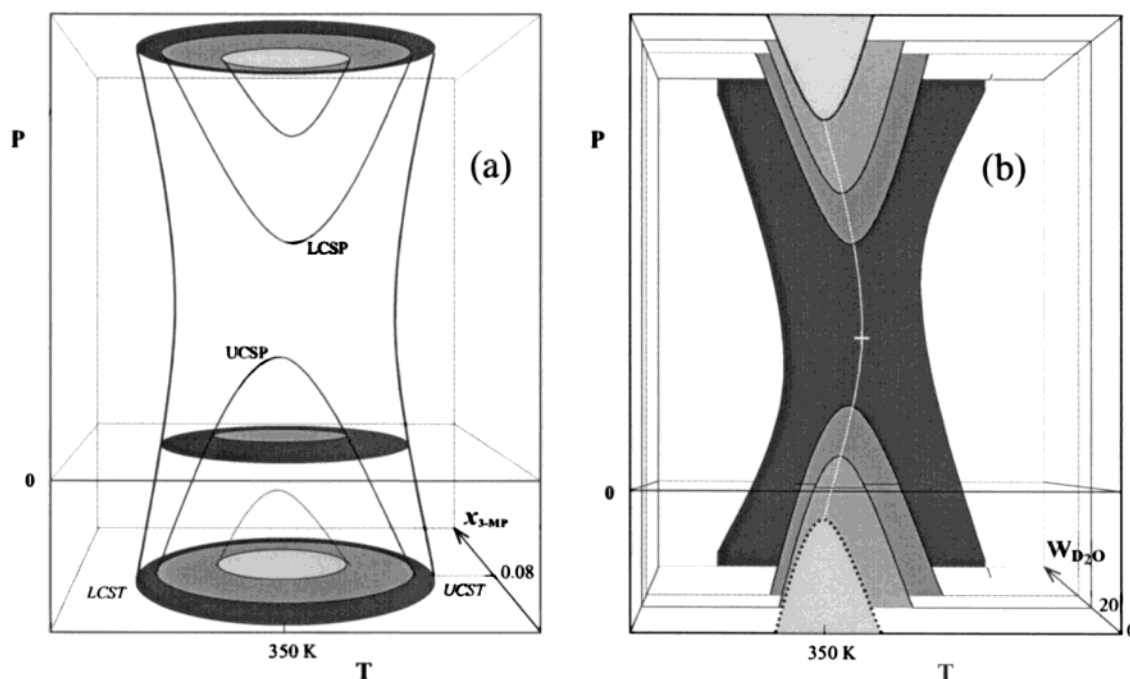


Figure 1. Two different 3-D representations of the phase diagram of 3-MP + water (H/D). (a) T - P - $x_{3\text{-MP}}$ for three distinct contents of D_2O in the mixed solvent ($\text{H}_2\text{O} + \text{D}_2\text{O}$). The two-phase regions are located inside the envelopes. Ellipses represent the T - x closed loops for three different pressures. Inner ellipses (light gray) and corresponding critical curves hold either for pure H_2O as solvent or any D_2O content of $0 < W_{\text{D}_2\text{O}}/\text{wt } \% < 17$. Intermediate ellipses stand for D_2O content of $17 < W_{\text{D}_2\text{O}}/\text{wt } \% < 21$. Outer ellipses (dark gray) and corresponding critical curves represent phase behavior either for pure D_2O as solvent or any D_2O content of $21 < W_{\text{D}_2\text{O}}/\text{wt } \% < 100$. In all cases there are four types of critical lines, i-CST, j-CSP, where $i, j = \text{U or L}$. All extrema of these lines correspond to double critical points. (b) Phase diagram at approximately constant critical concentration ($x \sim 0.08$) of 3-MP showing the evolution of the diagram as the deuterium content of water varies. The white line is the locus of temperature-double critical points (T-DCP) whose extremum (+) corresponds to the quadruple critical point (QCP).

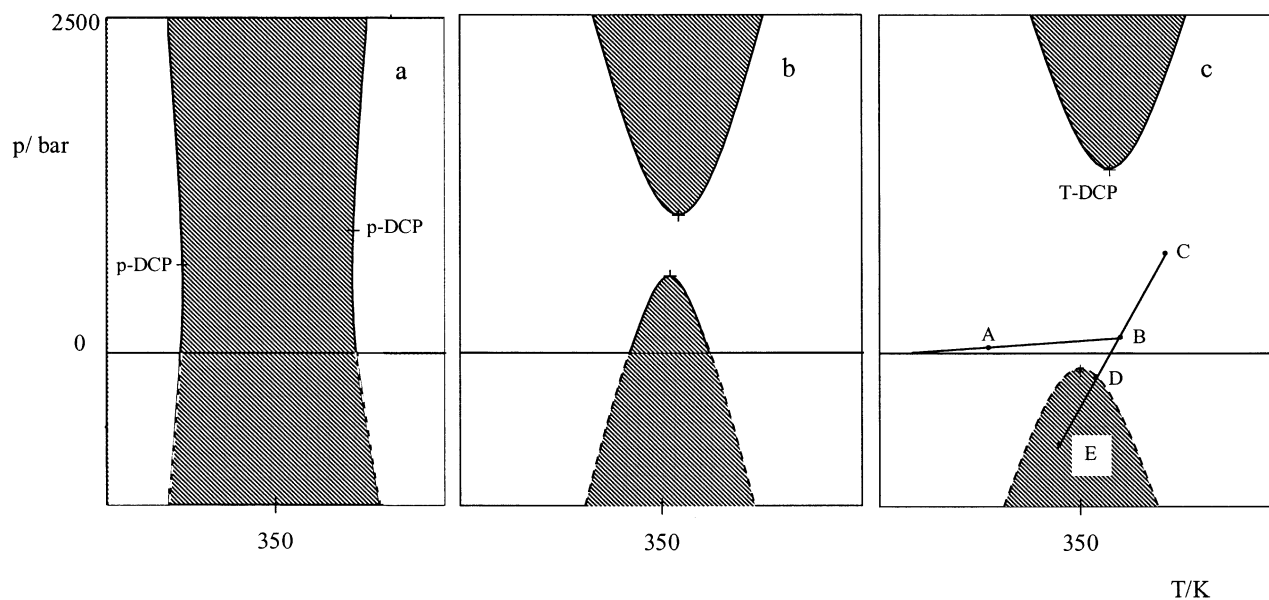


Figure 2. Schematic phase diagram of [water (H/D) + 3-MP] systems at critical $x_{3\text{-MP}} \sim 0.08$ and the typical course of a Berthelot T - p cycle¹³⁻¹⁵ (A-B-C-D-E) revealing the "hidden" region of absolute negative pressures. A, initial stage of solution with small gas bubble present; B, filling temperature; C, pre-pressurization stage; D, phase transition point; E, collapse of the metastable state. (a) D_2O as solvent; (b) $\text{H}_2\text{O}/\text{D}_2\text{O}$ mixture as solvent at about $W_{\text{D}_2\text{O}} = 20 \text{ wt } \%$; (c) H_2O as solvent. In all cases there are four types of critical lines. LCST-UCSP at low T and p ; LCST-LCSP at low T and high p ; UCST-UCSP at high T and low p ; UCST-LCSP at high T and p . T-DCP and p-DCP hold for temperature-double critical points and pressure-double critical points, respectively (see text). Critical lines drawn as dotted curves are in the metastable region of negative pressures.

p-DCPs one would expect a change in the sign of the excess volume, v^E , it is the excess enthalpy, h^E , that is the mixture's property that should present a zero value at T-DCPs. The existence of a unique critical point (quadruple critical point, QCP) can be inferred from the interpolation of already known (T, p, x) data. It corresponds to the intersection (or double cusp)

of the four critical lines (UCST, LCST, UCSP, and LCSP) in the T - p projection. It is a point where the mixture can accidentally be in an "ideal mixture state". We will return to this point later.

Tensioning liquids and liquid mixtures to the metastable region of absolute negative pressures¹¹⁻¹³ has recently received

renewed increased attention due mainly to several successful attempts to provoke phase separation under these conditions.^{14,15} So far, these have, however, been limited to polymeric solutions.

In this work, we present demixing phenomena data at absolute negative pressures for critical and close-to-critical concentrations of 3-MP in (H/D) water at conditions where the H/D ratio rises close to unity, and, thus, we span the T, p, x conditions of phase separation to about -250 bar. To the best of the authors' knowledge, the current study constitutes the first one where phase separation in nonpolymeric liquid mixtures has been provoked by diving into the absolute negative pressure region (metastable) of the phase diagram. Also, the high isotropic tensions here achieved constitute by far a record value (-350 bar) for macroscopic samples ($\sim 0.3\text{--}0.6\text{ cm}^3$). This is certainly due to the unique property of extraordinary adhesion of aqueous solutions of methylpyridine to Pyrex glass.¹⁶ It is found that the critical demixing of $\text{H}_2\text{O} + 3\text{-MP}$ in the low (and negative) pressure range can be provoked by isotropically stretching the critical mixture to a tension of about 210 bar. It is established that at temperatures in the neighborhood of 350 K , while a critical concentration of $3\text{-MP} + \text{D}_2\text{O}$ always presents phase separation irrespective of the applied pressure, when the solvent is pure H_2O , a miscibility window with a size of 1600 bar pops up. The results are interpreted by using a phenomenological approach that intimately relates the excess properties of the mixture to their critical lines. It is seen that, although the isotope effects on the phase diagram are quite dramatic, they can be explained by a solvent isotope independent excess enthalpy of mixing, which, however, changes sign as temperature is varied. The effect is thus entropic in nature, and the results of the phenomenological model show that a very small entropic shift upon solvent isotopic substitution is sufficient to set forth the large magnitude of the effect in the phase diagram.

2. Experimental Section

The experimental set-up and methodology used to achieve negative pressures and to detect phase transitions have already been described in great detail in previous reports.¹⁵ Only a brief description is provided here. The experiments were performed in thick-walled Pyrex-glass capillaries. The capillaries are sealed at both ends and initially the liquid (in the one-phase region) occupies almost the entire internal volume, leaving a very small dead volume gas phase (bubble). Then, the sample suffers a temperature–pressure Berthelot cycle^{11,13–15} induced by temperature change (see Figure 2). The cycle includes stages such as the “filling” point (at which, by thermal expansion, the liquid occupies the entire volume), the pre-pressurization point, the phase-transition point, and, finally, the collapse of the metastable state. A brief description follows with the visual aid provided by Figure 2c. At stage A the solution occupies partially the internal volume of the glass capillary and a small gas bubble is present at the top. Owing to expansion upon heating (along the vapor pressure line A–B) at B the liquid solution occupies the entire capillary's volume. The temperature at B is called the filling temperature, T_{fill} . Further heating provokes pressurization along a quasi-isochore of the liquid (B–C). Stage C is called the pre-pressurization point. On reversing the process by cooling (C–B–D–E) the liquid comes under tension when crossing B. This stretching of the liquid is only possible to occur if the liquid adheres well to the walls of the container. At D a phase transition occurs. Point E represents the maximum tension achieved. Further cooling will provoke the collapse of the metastable state and the return of the system to a stable condition (vapor pressure). In contrast to many other tensioning experi-

ments, macroscopically sized internal volumes of the glass containers (and, thus, of liquid samples) were used (typically, $\sim 0.3\text{--}0.6\text{ cm}^3$). Although one of the key factors for ensuring successful high tensions in a liquid is lost (the use of the smallest possible volume), the increase in the liquid's volume is necessary to guarantee visual detection of a phase transition, which induces strong turbidity or cloudiness in the liquid sample.

The Berthelot cycle is performed in a water bath controlled to better than $\pm 0.2\text{ K}$. Negative pressures are not directly measured but estimated through the thermal pressure coefficient of the liquid. A comprehensive critical discussion about this methodology can be found elsewhere.¹⁵ Phase transitions at negative pressures are obtained during the slow-cooling branch of the Berthelot cycle. This branch dictates a thermodynamic path which is a quasi-isochore for the liquid (C–B–D–E, Figure 2). The thermal pressure coefficient, γ_v , which is directly related to the isobaric thermal expansion coefficient (α_p) and the isothermal compressibility (K_T),

$$\gamma_v = \left(\frac{\partial p}{\partial T} \right)_v = -(\partial V / \partial T)_p / (\partial V / \partial p)_T = \frac{\alpha_p}{K_T} \quad (1)$$

is approximately constant along a single isochore, provided one works at temperatures far from the locus of maximum density of the aqueous solutions. Therefore, pressure can be easily obtained at any temperature once a reference (T_0, p_0) point is known. The point used is called the “filling” point ($T_{\text{fill}}, p_{\text{fill}}$), B in Figure 2, a point on the vapor pressure line of the liquid. Therefore

$$p = p_{\text{fill}} + \int_{T_{\text{fill}}}^T \gamma_v dT \approx p_{\text{fill}} + \gamma_v (T - T_{\text{fill}}) \quad (2)$$

Uncertainties in the achieved negative pressure arise mainly from uncertainties in T and in the equation of state (EoS) of the liquid (which determines the value of γ_v). Accurate p, v, T data for aqueous solutions of 3-MP are unknown but one should keep in mind that the mole fractions, x , of 3-MP used in this work are within the range $0.067\text{--}0.079$. Thus, in this limiting low concentration, it is acceptable to use the γ_v of water² slightly corrected for a linear interpolation (by mole fractions) between the values of water and 3-MP. The latter were estimated using the Sanchez-Lacombe EoS.¹⁷ Within our working temperature range ($320\text{--}360\text{ K}$), the shift in γ_v due to dissolution of about 8% (mol) of 3-MP in water never exceeds 3% , demonstrating this maximum value in the high-temperature limit. This is due to the fact that while 3-MP behaves like any other “normal” liquid (γ_v decreases with increasing temperature), water has an “abnormal” behavior where γ_v increases as temperature rises (up to $\sim 420\text{ K}$). In summary, when all corrections and their intrinsic uncertainties are considered, they cause an average error in pressure that should not exceed 5% . An additional correction due to the nonrigidity of the liquid's Pyrex glass container¹⁵ represents only about a 1% shift in the estimated pressure at the relatively high temperatures ($320\text{--}360\text{ K}$) of the current experiments.

Mixtures were gravimetrically prepared. 3-Methylpyridine from Aldrich (stated purity better than 99.5% by mass) was used as received. Normal water was doubly distilled and deionized (Millipore Co. equipment, Bedford, USA). D_2O was a donation of the Centro de Química Estrutural, IST, Lisbon, and arrived with a stated purity of 99.84% isotopic content. The purity was double-checked by high-precision density measure-

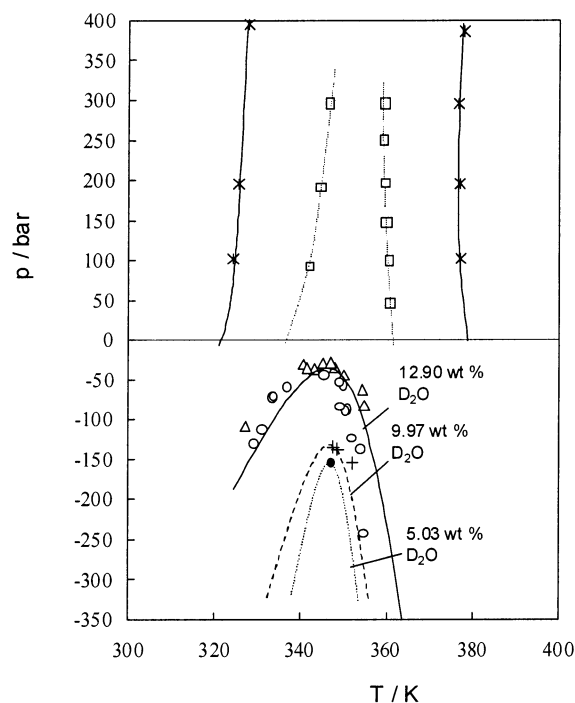


Figure 3. Metastable p - T loci of critical and close to critical demixing in [water (H/D) + 3-MP]. The phase diagram of the UCSP-type is located in the superheated region of absolute negative pressures. Δ , +, and \bullet , 30.4 wt % of 3-MP ($x_{3\text{-MP}}$ ranging from 0.0782 to 0.0788) in the mixed (H/D) solvent (12.90, 9.97, and 5.03, respectively, wt % of D_2O in (D_2O + H_2O)); \circ , 26.95 wt % of 3-MP ($x_{3\text{-MP}} = 0.0677$) in the mixed (H/D) solvent (14.93 wt % D_2O in (D_2O + H_2O)). The lines merely constitute a visual aid and have only been drawn for the critical concentration cases. The two-phase regions are located inside the envelopes. Also shown are experimental data (\square , $*$) found in the literature⁵ depicting low, positive pressure effects for the lowest available D_2O content (25 and 50 wt %, respectively).

ments (Anton-Paar vibrating tube densimeter). D_2O samples were further closed in sealed flasks under dried nitrogen atmosphere.

3. Results and Discussion

T - p phase transition curves were determined in the negative pressure region for near-critical concentrations (~ 30.4 wt % or ~ 7.88 – 7.82 % (mol) of 3-MP) and a slightly off-critical composition of 3-methylpyridine (~ 27.0 wt % or ~ 6.77 % (mol) of 3-MP). In the first cases, three distinct mixed (H/D) solvent water ranging from 12.9 to 5.0 wt % of D_2O in (D_2O + H_2O) were used, while in the latter only a single mixture with 14.9 wt % of D_2O was probed. The results are plotted in Figure 3. The two-phase regions are inside the envelopes. Although the envelopes drawn constitute mere visual guides, it is clear from the position of the data points that a maximum in the critical p - T line (*i.e.*, a T-DCP) is obtained for a temperature near 350 K. This agrees with all T-DCPs known for positive pressures (see Table 1),^{1,4–6,18} and it means that the temperature at which the T-DCP occurs is basically isotope (and pressure) independent. It has also been reported that the critical concentrations (at the LCSTs and UCSTs) of 3-MP, although not totally coincident for the two branches of the closed loop, are of about 0.08 (~ 30 wt %), irrespective of the isotopic content. All the above supports the concept that the isotopic label can be used as a thermodynamic variable. In view of this fact, a representation of the global phase diagram of this system can be obtained with a significant economy of parameters. The phase diagram

TABLE 1: Characteristics of the Atmospheric Pressure T - x Closed Loops of the System Water (H/D) + 3-MP^a

$w_{\text{D}_2\text{O}}$	$x_{1,c}^{\text{L}}$	$x_{1,c}^{\text{U}}$	T_c^{L} , K	T_c^{U} , K	ΔT , K	ref
1	0.0771	0.0996	311.65	390.15	78.50	1
0.24	0.0804	0.0827	338.74	360.80	22.06	7
0.17	0.0811 ^b	0.0811 ^b	349.80	349.80	0	37

^a $w_{\text{D}_2\text{O}}$ is the weight fraction of D_2O in (H_2O + D_2O). x_1 is the molar fraction of 3-MP in respect to [water (H/D) + 3-MP]. Lower (L) and upper (U) coordinates are shown. ΔT defines the size of the loop.

^b Estimated by nonlinear interpolation.

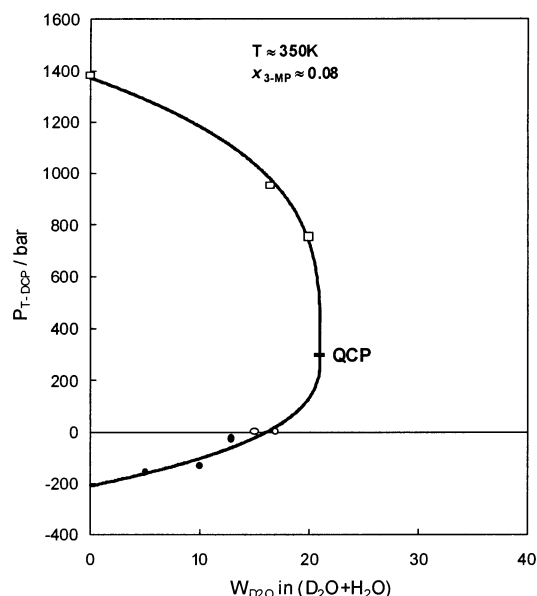


Figure 4. Simplified phase diagram of [(H/D) water + 3-MP] using a significant economy of field variables. The locus represents the solvent isotope effect on the pressure at which temperature-double critical points (T-DCP) appear ($T \sim 348.5$ K; $x_{3\text{-MP}} \sim 0.08$). The two-phase region is located to the right side of the line. Data points represent data both from this work (filled circles) and from the literature^{6,5} (open circles and open squares, respectively). The coordinates of the quadruple critical point (QCP) as well as the line were obtained through eq 3 (see also Figure 1b and its caption).

of the water ((H/D) + 3-MP), Figure 4, can thus be represented by a single line (a line of double critical points) at $x_{3\text{-MP}} \sim 0.08$ and $T \sim 350$ K. Figure 4 plots the locus of double critical points (T-DCPs) in a p versus weight percent of D_2O representation. This line is continuous from the positive to the negative side of pressure, because, obviously, invasions into the metastable states of negative pressures do not correspond to any discontinuity in the thermodynamics of a system. The two-phase region is located to the right side of the line. Note that the new data at negative pressures now permit a small safe extrapolation to the pure H_2O -state as solvent for this system (and what it would take to measure it experimentally).^{19,20} The isotope effect is impressive. It is shown that, while with normal water 3-MP has a window of miscibility of 1600 bar (high-pressure immiscibility at 1400 bar and metastable negative pressure immiscibility at about -200 bar), with the addition of a small amount of D_2O , that window vanishes completely at a quadruple critical point (QCP) (coordinates: 0.08 for x of 3-MP; 348.5 K; 299 bar; 21 wt % of D_2O in (D_2O + H_2O)). This point corresponds to the merge of the UCSP and LCSP lines (see Figure 1a,b). Similar to other studies of double criticality phenomena, we found that the coordinates of this QCP were best obtained from a least-squares fit provided by an unsymmetrical scaling fit⁹ of the form

$$\left| \frac{p - p_{\text{QCP}}^*}{p_{\text{QCP}}^*} \right| b = A \left(1 - \frac{W_{\text{D}_2\text{O}}}{W_{\text{D}_2\text{O}}^*} \right)^\alpha \quad (3)$$

where p is the locus of $p_{\text{T-DCP}}$, W is the weight percentage of D_2O in the solvent, and the asterisk refers to conditions which locate the QCP. In the case of the UCSP branch (lower part) $b = 1$, but, in the LCSP case, b is smaller in order to account for its larger amplitude. Within the context of treating the concentration of D_2O in water as a thermodynamic variable, the line in Figure 4 can also be labeled as the locus of lower-critical-solution-concentrations of D_2O .

Phenomenological Interpretation. Despite the unusual phase behavior of this system, we demonstrate below that we have succeeded in rationalizing it using a simplified g^{E} -model.¹⁰ The results show that the interpretation of the main features of the phase diagram can be performed under the assumption that the molar excess enthalpy of the solutions is isotope independent (but changing sign as temperature is varied), while entropic effects are sensitive to isotopic substitution. In liquid–liquid equilibrium, g^{E} -models are powerful tools for accessing relationships between the location of the phase diagram in the p, T, x space and excess properties of the mixture. This happens because phase separation occurs once a critical value for the excess molar Gibbs energy of the mixture (g^{E}) is attained, a fact which, in turn, is directly related to the excess molar enthalpy (h^{E}) and entropy (s^{E}) through its temperature dependence ($s^{\text{E}} = -\partial g^{\text{E}}/\partial T$, $h^{\text{E}} = \partial(g^{\text{E}}/T)/\partial(1/T) = -T^2\partial(g^{\text{E}}/T)/\partial T$, and $g^{\text{E}} = h^{\text{E}} - Ts^{\text{E}}$). g^{E} is a function of T , p , and x , and, therefore, pressure (or tension) can also provoke phase splitting. The relevant property to be analyzed when phase separation is being studied at constant temperature is, thus, the excess molar volume, $v^{\text{E}} = \partial g^{\text{E}}/\partial p$. Phase diagrams in their T – x projections are usually better known than those in their p – x counterparts. The current system under investigation does not constitute an exception to this rule. Consequently, most of the discussion below focuses on the temperature dependence of g^{E} .

One of the peculiar features of this system is that while the closed-loop T – x phase diagram is extremely shifted to very low molar fractions^{1,7} of 3-MP (the critical molar fractions, upper and lower, are only ~ 0.08), its excess functions (including the excess molar volume, v^{E}) are fairly symmetrical^{21–24} in respect to their composition dependence. Such behavior resembles that of (polymer + small molecule) solutions⁹ and has also very recently been found in solutions of room-temperature ionic liquids with conventional solvents.²⁵ Therefore, to account for the extreme asymmetry of the phase diagram in its (T – x) projection, a “polymer-solution-like” g^{E} -model²⁶ ought to be used. This is done in a similar vein to that suggested by Schneider²⁷ for the treatment of molecular solutions of this type. An additional important experimental fact to take into consideration is that, within experimental precision, the excess enthalpies of mixtures of 3-MP with H_2O and D_2O at their critical molar fraction (0.08) are indistinguishable.²⁴ At this critical concentration (where phase separation may occur) the two values of the excess enthalpy merely differ by 0.35% (-559 and -557 J mol^{-1} for H_2O and D_2O , respectively), while the experimental uncertainty, although low, amounts to about $\pm 10 \text{ J mol}^{-1}$.

Let us define component 1 as the solute ($1 \equiv 3\text{-MP}$) and component 2 as the solvent ($2 \equiv \text{water (H/D)}$). Independent of the degree of isotopic substitution in the solvent, the system will always be treated in the binary mixture approximation. Due to entropic effects originated at the large difference in size between the mixture’s components²³ ($v_1/v_2 \cong 5$), the change in

the molar Gibbs energy on mixing, at a fixed pressure, can be defined as

$$\Delta g_{\text{m}} (\text{J mol}^{-1}) = RT[x_1 \ln \varphi_1 + x_2 \ln \varphi_2 + \chi(T)x_2\varphi_1] \quad (4)$$

$$\varphi_1 = \frac{rx_1}{rx_1 + x_2} \quad (5)$$

$$\varphi_2 = \frac{x_2}{rx_1 + x_2} \quad (6)$$

where x_i stands for the molar fraction of component i , r defines the ratio of their sizes ($r = 5$ in this case), and φ_i can be interpreted either as a temperature-independent volume fraction or a segment fraction²⁶ in a lattice model.²⁸ In this type of model the structure of the solution is represented by a three-dimensional lattice, each cell of which contains either a molecule or part of a molecule. If the mixture is composed of small, similar-sized molecules, each cell contains a single molecule. When one compares, statistically, the number of configurations available when the unlike species are separated with the situation where they are mixed, one finds that the entropy increase originating at this interaction-free mixing is $\Delta s_{\text{m}} = -R[x_1 \ln x_1 + x_2 \ln x_2]$. If one component is much greater than the other each cell contains what is called a segment of that larger molecule, and its molecules occupy several cells. Therefore, there is now a statistical restriction to the location of the segments of the long molecule—the segments must run contiguously through the lattice. Application of the same statistical framework leads to the result that, in this case, the interaction-free mixing resulting solely from the different number of available arrangements in the separated and mixed states is $\Delta s_{\text{m}} = -R[x_1 \ln \varphi_1 + x_2 \ln \varphi_2]$. The corresponding change in the Gibbs energy due to this interaction-free mixing is $\Delta g_{\text{m}} = -T\Delta s_{\text{m}} = RT[x_1 \ln \varphi_1 + x_2 \ln \varphi_2]$ (see first two terms of the right-hand side of eq 4). $\chi(T)$ is the energy parameter that takes into account the interaction between unlike molecules. More specifically, it can be interpreted as the interchange energy involved in breaking like-segment bonds to form unlike-segment ones. $\chi(T)$ produces, thus, a reduced interchange Gibbs energy of mixture. In accordance with others,²⁹ we have identified this excess of Gibbs energy over that statistically produced merely by counting configurations available in the dissolved and undissolved states, with values of $\chi \neq 0$. Although our model is simply phenomenological, in eq 4 one can recognize the purely entropic part arising from the statistics of mixing, the two first terms, and the excess-interchange one, g^{EI} , which can have entropic and enthalpic contributions. χ can generally be temperature, pressure, and composition dependent. For the present purposes, we consider it only dependent upon temperature.

Equation 4 can be rearranged, obtaining

$$\frac{\Delta g_{\text{m}}}{(rx_1 + x_2)} = \Delta g_{\text{m}}^* (\text{J seg mol}^{-1}) = RT \left[\frac{\varphi_1}{r} \ln \varphi_1 + \varphi_2 \ln \varphi_2 + \chi(T)\varphi_1\varphi_2 \right] \quad (7)$$

where the asterisk holds for a quantity expressed now per unit molar volume or unit segment-mole. Note that the last term of the third member of eq 7 is the excess-interchange molar Gibbs energy expressed per segment-mole, $g^{\text{EI}*}$. Within the simplicity of the model, this interchange Gibbs energy is symmetrical (and parabolic) in the segment fraction space. Therefore, for the

“symmetrical” model, one can re-express the excess-interchange Gibbs energy as

$$g^{\text{EI}}(\text{J mol}^{-1}) = RT[(rx_1 + x_2)\chi(T)\varphi_1\varphi_2] = RT\chi(T)\frac{rx_1x_2}{rx_1 + x_2} \quad (8)$$

which is now asymmetrical in the molar fraction space. Any excess function, L^{E} , can thus be expressed per unit mole or unit segment-mole by the simple transformation

$$L^{\text{E}*} = \frac{L^{\text{E}}}{(rx_1 + x_2)} \quad (9)$$

Note that eqs 4–9 reduce themselves to their more common form if r is set as unity.

From this point on, obtaining the other excess functions is straightforward. For instance

$$h^{\text{E}}(\text{J mol}^{-1}) = RT[(rx_1 + x_2)\zeta(T)\varphi_1\varphi_2] = RT\zeta(T)\frac{rx_1x_2}{rx_1 + x_2} \quad (10)$$

where, by definition

$$\zeta(T) = -T\frac{d\chi}{dT} \quad (11)$$

If one uses the thermodynamic conditions dictating the critical phase separation,^{10,26} then one concludes that critical demixing occurs at a composition of

$$x_{1,\text{c}} = \frac{1}{1 + r^{3/2}}, \quad \varphi_{1,\text{c}} = \frac{1}{1 + r^{1/2}} \quad (12)$$

and at a critical value for the interaction parameter given by

$$\chi_{\text{c}} = \frac{1}{2}\left(1 + \frac{1}{r^{1/2}}\right)^2 \quad (13)$$

Again, note that for $r = 1$ the critical demixing occurs at the equimolar composition and when the critical interaction parameter reaches a value equal to 2. In the present case ($r = 5$), and with this “symmetrical” model in the segment-mole space, critical demixing occurs for

$$x_{1,\text{c}} = 0.0821; \quad \varphi_{1,\text{c}} = 0.309; \quad \chi_{\text{c}} = 1.047 \quad (14)$$

Despite the crudeness of the “symmetrical” model, it is worth emphasizing how well it predicts the experimental LCST and UCST critical molar fractions value for this mixture (~ 0.08 ; see also Table 1). This is merely obtained by taking into account entropic effects due to the difference in size between the mixture’s components. Strictly speaking, no mixture follows truly “symmetrical” behavior. In other words, the interaction parameter, χ , as defined by eq 7, is not merely temperature dependent but also composition (and pressure) dependent, $\chi = \chi(T, p, \varphi)$. In a previous work,¹⁰ we showed that the simplest, theoretically sound model capable of generating all “basic”³⁰ types of L–L phase diagrams is one in which

$$\chi(T, p) = D(T, p)\Sigma(\varphi) = d_0(p) + \frac{d_1(p)}{T} - d_2 \ln T \quad (15)$$

where $\Sigma(\varphi)$, a Redlich–Kister type of expansion to take care of the asymmetry of the excess functions in the composition

space, is set equal to unity for the sake of simplicity. The parameters d_0 , d_1 , and d_2 , where the first two are generally pressure dependent, set the temperature dependence of the interaction parameter. Consequently, at a given pressure, critical demixing occurs whenever

$$\chi = \chi_{\text{c}} = D(T) = d_0 + \frac{d_1}{T} - d_2 \ln T \quad (16)$$

where χ_{c} is a number given by eq 13 for this “symmetrical” model (see also eq 14). A maximum of two solutions in T (the critical temperatures) are obtained from eq 16. Phase splitting occurs for values of χ greater than χ_{c} . Parameters d_1 and d_2 are intimately related to the excess enthalpy of the mixture since (see eqs 10 and 11)

$$\zeta(T) = \frac{d_1}{T} + d_2 \quad (17)$$

and they set forth the type of temperature dependence of both g^{E} and h^{E} , eqs 16 and 17, respectively. The parameter d_0 is related to the magnitude of the excess entropy of the mixture (and thus of the excess Gibbs energy as well), $T_{\text{S}}^{\text{E}} = h^{\text{E}} - g^{\text{E}}$.

Within the limits of validity of this “symmetrical” model, it is now easy to obtain the three parameters provided that critical temperatures of demixing and the excess enthalpy at a single (and any) temperature are known. Experimental excess enthalpy values²⁴ are compared with calculated ones via eqs 10 and 17. This permits us to set a first relation between d_1 and d_2 . The second relation arises from the fact¹⁰ that at T-DCPs ($dT_{\text{c}}/dp = \infty$), which is the merging point of LCST and UCST, $h^{\text{E}} = 0$. Here, eq 16 provides a single solution. At the temperature where the T – x closed-loop shrinks to a single dot ($\sim (T_{\text{c}}^{\text{U}} + T_{\text{c}}^{\text{L}})/2$), eq 17 is equal to zero. These two relations fix the values of d_1 and d_2 . d_0 is then obtained for each closed loop (see Table 1 and references therein) by using eq 16 for the upper and lower critical temperatures.

To fine tune the match between the model and the experimental results (of closed loops and excess properties), we have adopted a more realistic model which is no longer “symmetrical”. The perturbation in respect to the above-mentioned simple model is minor and simply corresponds to avoiding setting the function $\Sigma(\varphi) = 1$. This function of composition is merely a Redlich–Kister expansion. Nevertheless, the implications in the algebra of the calculations arising from this slight correction are not negligible. In the Appendix one can find the details of the “asymmetrical” model.

Calculated (spinodal) and fitted experimental (binodal) results are plotted in Figure 5 for atmospheric pressure. The model’s parameters were obtained in a similar fashion as explained for the “symmetrical” case. The good agreement between the model’s calculations and the experimental data can be judged by the match of the critical temperatures (and concentrations) in all three cases. Numerical values for the parameters are reported in Table 2. Note that the phase behavior shift induced by isotopic substitution is rationalized simply by varying (linearly) the d_0 parameter (isotope dependent) with respect to the weight percent of D₂O but maintaining d_1 and d_2 fixed (isotope independent).

The model can now also be used to produce at 298.15 K and 1 bar the excess functions of the mixture (see eqs 8, 10, 11, and 15). Excluding the excess molar volumes,²³ which are not analyzed in detail within the context of the present work,³¹ while the h^{E} s are known for both H₂O and D₂O as solvents,²⁴ g^{E} is only known for the first case.²¹ The experimental excess

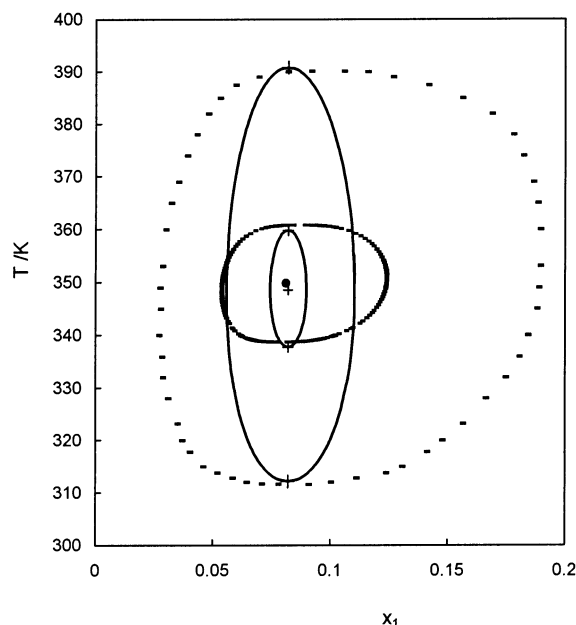


Figure 5. Closed-loop T - x phase diagrams at atmospheric pressure for three solutions of [(H/D) water + 3-MP] differing in the solvent H/D content. x_1 is the mole fraction of 3-MP. Concentrations (wt %) of D_2O in $(H_2O + D_2O)$ as one moves from the outer phase diagram to the inner one are 100, 24, and 17, respectively. (—) fitted experimental data for the binodals taken from refs 1, 7, and 37 respectively for 100, 24, and 17 wt % of D_2O in the mixed solvent. Full lines represent the results of the model's calculations for the spinodal lines. (+) Critical points as calculated from the model.

TABLE 2: Parameters of the “Asymmetrical” Model (see Eq 15 and Appendix) at Atmospheric Pressure^a

W_{D_2O}	d_0	d_1 , K	d_2	B_0	B_1	B_2	B_3
100	61.428(5)	-3076.2(5)	8.8271(2)	-0.125	0.12	0.40	0.30
24	61.377(2)	-3076.2(5)	8.8271(2)	-0.125	0.12	0.40	0.30
17	61.372(8)	-3076.2(5)	8.8271(2)	-0.125	0.12	0.40	0.30
0	61.360(1) ^b	-3076.2(5)	8.8271(2)	-0.125	0.12	0.40	0.30

^a W_{D_2O} represents the weight percent of D_2O in $(H_2O + D_2O)$.
^b Obtained by linear extrapolation of the other three values to $W_{D_2O} = 0$. For a perfect match between the calculated and experimental extremum of the g^E function for $(H_2O + 3-MP)$ a nonlinear extrapolation to a value of 61.205 would have to be used.

enthalpies of mixtures of $H_2O + 3-MP$ are basically indistinguishable from those of $D_2O + 3-MP$ in the whole concentration range. They differ by 0.35% at the critical concentration $x_{1,c} = 0.08$ and by 2.5% at the common extremum $x_1 = 0.43$. Figure 6 compares the experimental and calculated results for three excess functions for the case of the $(H_2O + 3-MP)$ system. It is highly rewarding to verify that the model successfully predicts all three excess functions with reasonable precision. Note that in comparing the extrema values between calculated and experimental excess functions, differences never exceed 4%. This fact substantiates the significance of the parameters. Despite being obtained with the aid of totally independent experimental information, i.e., L - L phase separation, the model's parameters are able to correctly estimate the deviations from ideality of the solutions.

Figure 7 shows the predicted (model) global behavior of the extrema values of the excess functions as the isotopic label on the solvent varies. All available experimental information on both the phase transitions and the excess properties can simply be rationalized by an isotope-independent h^E and a s^E that becomes slightly more negative as D_2O replaces H_2O . It is remarkable how such a subtle change in the entropy of the

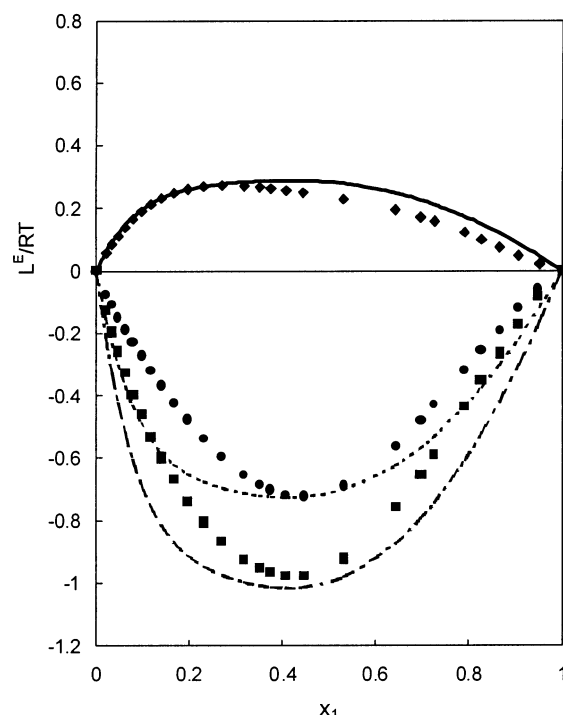


Figure 6. Experimental and calculated (model) excess properties for the $(H_2O + 3-MP)$ system at 298.15 K and nominal 1 bar pressure compared. x_1 is the mole fraction of 3-MP. $L^E = g^E$ (diamonds), h^E (circles), or Ts^E (squares). Filled symbols hold for experimental data (g^E ,²¹ h^E ,²⁴ and $Ts^E = h^E - g^E$), while lines refer to model calculations (—, g^E ; ···, h^E ; -·-, Ts^E).

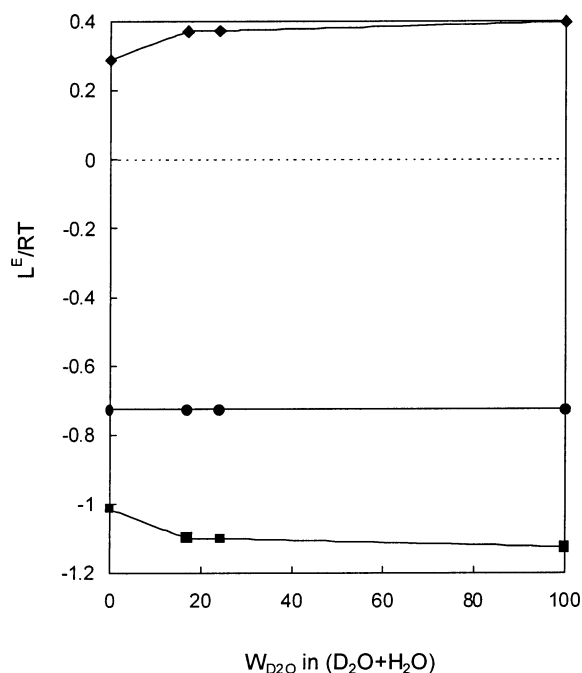


Figure 7. Isotopic (H/D) dependence of the extrema of excess properties at 298.15 K and nominal 1 bar pressure from model calculations. $L^E = g^E$ (diamonds), h^E (circles), or Ts^E (squares).

mixture can provoke such distinct phase behavior as the solvent isotopic content varies.

A final comment about the phenomenological analysis of this system is pertinent. This has to do with the relationship between the slope (and curvature) of the T - p critical lines and the excess functions of the mixture. It was originally shown by Prigogine and Defay³² and later revisited and discussed by others^{9,10,27,33}

that the slope of the T - p critical loci is intimately related to the second derivative with respect to composition of the mixture's volume and enthalpy through

$$\left(\frac{dT}{dp}\right)_c = \lim_{\substack{T \rightarrow T_c \\ x \rightarrow x_c}} \frac{\partial^2 v_M / \partial x^2}{\partial^2 s_M / \partial x^2} = \lim_{\substack{T \rightarrow T_c \\ x \rightarrow x_c}} T \frac{\partial^2 v_M / \partial x^2}{\partial^2 h_M / \partial x^2} \quad (18)$$

It is also well-known that, in order for e.g. a LCST to occur, it is necessary that

$$\left(\frac{\partial^2 h_M}{\partial x^2}\right)_c = \left(\frac{\partial^2 \Delta h_{\text{mix}}}{\partial x^2}\right)_c = \left(\frac{\partial^2 h^E}{\partial x^2}\right)_c > 0 \quad (19)$$

whereas, for an UCST, the above inequality is of opposite sign. Any liquid-liquid critical line has a given T - p slope, and therefore the phase diagram may also be represented by p - x cuts (at constant temperature). From this perspective, any phase separation can be labeled as either the UCSP-type or the LCSP one (isothermal pressurization provokes phase separation). For a LCSP to occur, it is necessary that

$$\left(\frac{\partial^2 v_M}{\partial x^2}\right)_c = \left(\frac{\partial^2 \Delta v_{\text{mix}}}{\partial x^2}\right)_c = \left(\frac{\partial^2 v^E}{\partial x^2}\right)_c < 0 \quad (20)$$

whereas, for a UCSP, the above inequality is of opposite sign. Any liquid-liquid critical line should therefore more correctly be labeled as (i-CST, j-CSP), where i, j = U or L. There are, thus, a total of four possibilities (see Figures 1 and 2 and their caption), all of which are present in the current pair (H_2O or D_2O + 3-MP) of systems since phase separation can be brought about by varying either temperature or pressure.

Therefore, the sign of $(dT/dp)_c$ establishes that of the second derivatives of the molar enthalpy and volume of the mixture in respect to composition (and vice versa). Although it entails some loss of generality, it is preferable to relate the slope of the critical loci to the excess functions themselves rather than to their second derivatives. If the distinct excess functions strictly conform to each other in respect to their composition dependence, then, independent of any anomalies such as inflection points, the following relation should also be verifiable:

$$\left(\frac{dT}{dp}\right)_c \cong \frac{T_c v_c^E}{h_c^E} \cong \frac{T_c v_{\text{ext}}^E}{h_{\text{ext}}^E} \quad (21)$$

where the subscripts c and ext refer to critical composition and the composition at which the excess property presents an extremum, respectively. The above-mentioned simplification holds valid if the excess Gibbs energy of mixing does not present cross temperature- or pressure-composition terms; the currently adopted model meets these conditions. Therefore, for instance, both a T-DCP and a hypercritical region occur at T where $h^E = 0$ because, here, $dT_c/dp = \infty$. Using eqs 10 and 17 this occurs for $T = -d_1/d_2 = 348.50$ K. This is shown in detail in Figure 8 along with the predicted change in sign and magnitude of h^E as the temperature is varied. This contrasts with g^E , which is always found to be positive within the same temperature range. Interestingly, s^E is negative only up to a temperature of about 385 K, becoming significantly positive at 400 K. Within the framework of the model, the excess isobaric heat capacity, C_p^E , which is the temperature derivative of h^E , is a composition-dependent but temperature- and isotope-independent quantity with a maximum value of $33.7 \text{ J mol}^{-1} \text{ K}^{-1}$ at a composition $x_1 = 0.41$.

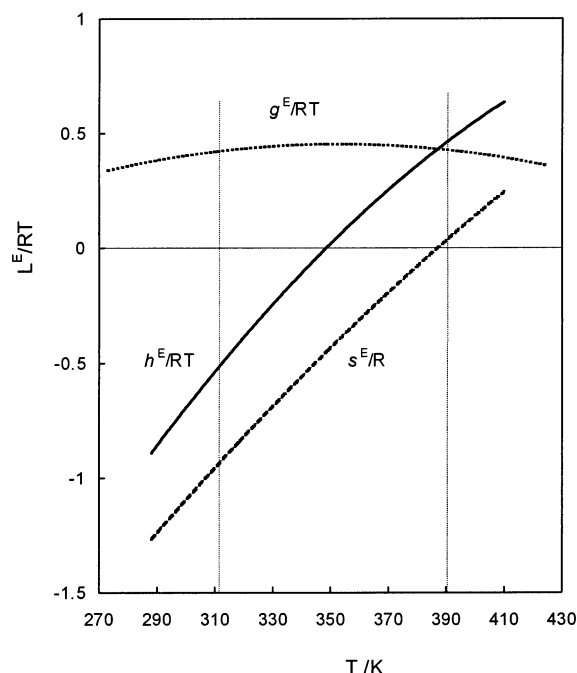


Figure 8. Temperature dependence of the extremum of excess properties at $p = 1$ bar from model calculations. $L^E = g^E$ (···), h^E (—), or Ts^E (---). Vertical lines represent the temperature-immiscibility window when the solvent is D_2O .

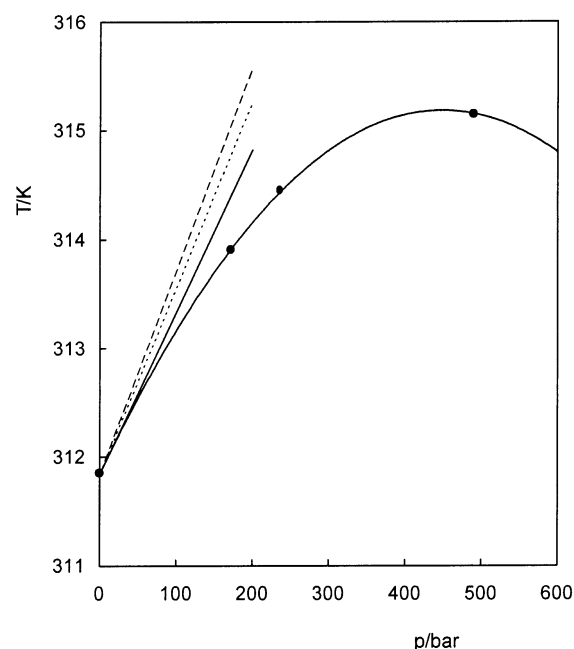


Figure 9. Close up of the pressure dependence of the LCST transition for D_2O + 3-MP. ●, experimental data taken from ref 5. The full curve represents a polynomial that fits the experimental data, while the full straight line depicts its slope for the nominal limiting $p = 0$ value. Dotted and dashed lines represent the calculated slope from eq 21 in the first and second approximate equalities, respectively.

Since both h^E and v^E are experimentally well-known (see above) at 298.15 K and a nominal pressure of 1 bar, it is possible to estimate the value of the slope of the critical line (of type LCST, UCSP) in the neighborhood region of this datum point. In the case of D_2O as solvent (T_c (1 bar) = 311.65 K) the experimental $dT_c/dp = (1.49 \pm 0.10) \times 10^{-2} \text{ K bar}^{-1}$ (see ref 5 and Figure 9). The two estimates given by eq 21 originate values of $(1.71 \pm 0.10) \times 10^{-2}$ and $(1.86 \pm 0.10) \times 10^{-2} \text{ K bar}^{-1}$, respectively. Both are in good agreement with the

experimental slope (see Figure 9). Were h^E and v^E strictly conformal, the two estimates would coincide. When one considers this pair of systems in the high-pressure region, the critical lines (see Figures 1, 2, and 9) are no longer of the UCSP type but rather of the LCSP one. This means that, while pressure increases, either the excess volume changes its sign or, alternatively, the curvature of the excess volume at the critical composition changes sign. In a future contribution³¹ we will analyze in detail the role of the excess volume (and its isotopic dependence) on the p - x projection of the phase diagram.

Theoretical analyses of this type of systems at a molecular level mainly focus on the characteristics of the MP–water interaction.^{34–36} All of them stress the importance of the shift in the strength of the hydrogen bond formed in the methylpyridine–water association upon a change of position of the methyl-substituted pyridines and/or solvent isotopic substitution. While one set of theories establishes that immiscibility increases upon hydrogen bond strengthening between unlike molecules, the other concludes the opposite. The current study does not shed much light on this issue, but it permits us to raise another one. It is well documented by thermodynamic arguments (and well illustrated by the current study) that the driving force for provoking a phase separation is the attainability of a critical value for the excess Gibbs energy, above which phase splitting occurs (Figure 8, although drawn for the extremum of the functions, clearly depicts this phenomenon). In turn, this critical value is intimately related to two others (one for the excess enthalpy and the other for the excess entropy) through a delicate balance ($g^E = h^E - Ts^E$). The bottom line is that it is not only the absolute value of the mixture’s property (and, thus, likewise, the strengthening or weakening of the interaction between unlike molecules) that triggers the phase transition but rather its relative value in comparison to its counterpart in the reference pure-components-state. When one compares H₂O with D₂O as solvents for the methylpyridine mixtures, that reference state changes. Neither the energy nor the entropy is identical for pure H₂O and D₂O. At a certain common temperature, the number and intensity of the several types of hydrogen bonding associating water molecules are distinct for the two isotopic forms of water. Therefore, the molecular analyses should focus on the difference between the intensity and number of the *heteromolecular* hydrogen bonds in the mixtures in H₂O and D₂O minus that of the *homomolecular* hydrogen bonds in pure H₂O and D₂O. Another relevant interaction is that between H₂O (or D₂O) and the hydrophobic part of MP. Obviously, this type of interaction does not exist in the reference pure-components-state. If one assumes that H₂O and D₂O behave distinctly in respect to their interaction with the hydrophobic part of MP, then, this effect cannot be neglected, and, thus, it also has a role in the interpretation of the difference in phase behavior upon isotopic substitution. In light of the thermodynamic experimental evidence available, and irrespective of the issue of strengthening/weakening of the interactions brought about by H/D isotopic substitution, the above-mentioned double difference, “H” minus “D”, mixture minus reference pure-components-state, in the averaged overall enthalpic contribution, seems to cancel out at the critical concentration of 3-MP, since the excess enthalpy is isotope-independent to very good approximation. This must be taken into account.

Acknowledgment. We are thankful to Dr. Gábor Jancsó, Atomic Energy Research Institute, Budapest, for helpful discussions. This work was financially supported by FCT under contract POCTI # 34955/EQU/2000.

Appendix. The “Asymmetrical” Model

Taking eq 15, now with the function $\Sigma(\varphi)$ given by a typical Redlich–Kister expansion

$$\Sigma(\varphi) = 1 + B_0(2\varphi_1 - 1) + B_1(2\varphi_1 - 1)^2 + B_2(2\varphi_1 - 1)^3 + B_3(2\varphi_1 - 1)^4 + \dots \quad (\text{A1})$$

the excess segment molar Gibbs energy now reads

$$g^{E*} = RTD(T)\varphi_1(1 - \varphi_1)[1 + B_0(2\varphi_1 - 1) + B_1(2\varphi_1 - 1)^2 + B_2(2\varphi_1 - 1)^3 + B_3(2\varphi_1 - 1)^4] \quad (\text{A2})$$

Equations 16 and 17 still hold merely by replacing χ by D (which is only a function of T).

Solutions can be found by using the conditions for the spinodal locus

$$\frac{\partial^2 \left(\frac{1}{RT} \Delta g_m^* \right)}{\partial \varphi_1^2} = 0 \quad (\text{A3})$$

and those for the critical point

$$\frac{\partial^2 \left(\frac{1}{RT} \Delta g_m^* \right)}{\partial \varphi_1^2} = \frac{\partial^3 \left(\frac{1}{RT} \Delta g_m^* \right)}{\partial \varphi_1^3} = 0 \quad (\text{A4})$$

Consequently, eqs A3 and A4 now take the forms

$$\frac{\partial^2 \left(\frac{1}{RT} \Delta g_m^* \right)}{\partial \varphi_1^2} = \frac{1}{r} \frac{1}{\varphi_1} + \frac{1}{1 - \varphi_1} + D(T)(2K_2 + 6K_3\varphi_1 + 12K_4\varphi_1^2 + 20K_5\varphi_1^3 + 30K_6\varphi_1^4) = 0 \quad (\text{A5})$$

$$\frac{\partial^3 \left(\frac{1}{RT} \Delta g_m^* \right)}{\partial \varphi_1^3} = -\frac{1}{r} \frac{1}{\varphi_1^2} + \frac{1}{(1 - \varphi_1)^2} + D(T)(6K_3 + 24K_4\varphi_1 + 60K_5\varphi_1^2 + 120K_6\varphi_1^3) = 0 \quad (\text{A6})$$

with

$$K_2 = -1 + 3B_0 - 5B_1 + 7B_2 - 9B_3 \quad (\text{A7})$$

$$K_3 = -2B_0 + 8B_1 - 18B_2 + 32B_3 \quad (\text{A8})$$

$$K_4 = -4B_1 + 20B_2 - 56B_3 \quad (\text{A9})$$

$$K_5 = -8B_2 + 48B_3 \quad (\text{A10})$$

$$K_6 = -16B_3 \quad (\text{A11})$$

Note that solving the case corresponding to the “symmetrical” model in this segment-mole space means that $K_{i \geq 3} = 0$ and $K_2 = -1$. Consequently, solutions of eqs A5 and A6 are identical to those of eqs 12 and 13, respectively.

References and Notes

- (1) Cox, J. D. *J. Chem. Soc.* **1952**, 4606.
- (2) Rowlinson, J. S.; Swinton, F. L. *Liquids and Liquid Mixtures*, 3rd ed.; Butterworth: London, 1982.
- (3) Schneider, G. M. *Ber. Bunsen-Ges. Phys. Chem.* **1972**, 76, 325.
- (4) Timmermans, J.; Lewin, J. *Discuss. Faraday Soc.* **1953**, 15, 195.
- (5) Schneider, G. Z. *Phys. Chem. Neue Folge* **1963**, 37, 333; 39, 187.
- (6) Narayanan, T.; Kumar, A. *Phys. Rep.* **1994**, 249, 135.

- (7) Narayanan, T.; Kumar, A.; Gopal, E. S. R. *Phys. Lett. A* **1991**, 155, 276.
- (8) Sidebottom, D. L.; Sorensen, C. M. *Chem. Phys. Lett.* **1988**, 151, 489. Narayanan, T.; Kumar, A.; Gopal, E. S. R. *Phys. Lett. A* **1990**, 144, 371. Prafulla, B. V.; Narayanan, T.; Kumar, A. *Phys. Lett. A* **1992**, 164, 443. Prafulla, B. V.; Narayanan, T.; Kumar, A. *Phys. Rev. A* **1992**, 46, 7456.
- (9) Rebelo, L. P. N.; Visak, Z. P.; de Sousa, H. C.; Szydlowski, J.; de Azevedo, R. G.; Ramos, A. M.; Najdanovic-Visak, V.; Nunes da Ponte, M.; Klein, J. *Macromolecules* **2002**, 35, 1887.
- (10) Rebelo, L. P. N. *Phys. Chem. Chem. Phys.* **1999**, 1, 4277.
- (11) Henderson, S. J.; Speedy, R. J. *J. Phys. Chem.* **1987**, 91, 3062. Henderson, S. J.; Speedy, R. J. *J. Phys. Chem.* **1987**, 91, 3069. Zheng, Q.; Durben, D. J.; Wolf, G. H.; Angell, C. A. *Science* **1991**, 254, 829.
- (12) *Liquids Under Negative Pressure*; Imre, A. R., Maris, H. J., Williams, P. R., Eds.; NATO Science Series; Kluwer Academic Publishers: Dordrecht, 2002. Debenedetti, P. G. *Metastable Liquids*; Princeton University Press: Princeton, NJ, 1996.
- (13) Imre, A.; Martínás, K.; Rebelo, L. P. N. *J. Non-Equilibrium Thermodyn.* **1998**, 23, 351. Veiga, H. I. M.; Rebelo, L. P. N.; Nunes da Ponte, M.; Szydlowski, J. *Int. J. Thermophys.* **2001**, 22, 1159.
- (14) Imre, A.; Van Hook, W. A. *Chem. Soc. Rev.* **1998**, 27, 117. Imre, A.; Van Hook, W. A. *J. Polym. Sci. B: Polym. Phys.* **1994**, 32, 2283.
- (15) Rebelo, L. P. N.; Visak, Z. P.; Szydlowski, J. *Phys. Chem. Chem. Phys.* **2002**, 4, 1046. Visak, Z. P.; Rebelo, L. P. N.; Szydlowski, J. *J. Chem. Educ.* **2002**, 79, 869.
- (16) Narayanan, T.; Kumar, A.; Gopal, E. S. R.; Beysens, D.; Guenoun, P.; Zalczer, G. *Phys. Rev. E* **1993**, 48, 1989.
- (17) Sanchez, I. C.; Lacombe, R. H. *Macromolecules* **1978**, 11, 1145.
- (18) Szydlowski, J. *Nukleonika* **1998**, 43, 423.
- (19) It should be noted that although Figure 3 represents a single run where the negative pressure for the phase transition reaches -250 bar, this value is not common. It is well-known that maximum experimental tensions achieved in liquids cannot be strictly reproduced from run to run even with the same sealed capillary. In attempts with pure H_2O acting as solvent, we were unable to reach tensions without cavitation higher than -180 bar. Thus, we were unable to obtain a direct measurement of critical demixing in this case.
- (20) In some experiments, higher tensions than those corresponding to pressures of -200 bar were held for long periods of time, despite the fact that the system had already entered the two-phase region. In one a pressure $p = -353 \pm 20$ bar was reached. In another, one single Berthelot run revealed, first, the phase separation between the top 3-MP rich phase and the bottom H/D water rich one and, afterwards, at higher tensions, turbidity (due to strong heterogeneity) in the top phase. This heterogeneity was certainly originated at the diffusion of more 3-MP from the bottom to the upper phase, a process which has an increasing driving force as tension raises. The system only collapsed and relaxed to total equilibrium at a dive inside the metastable 2-phase region as deep as 76 bar of tension.
- (21) Abe, J.-I.; Nakanishi, K.; Touhara, H. *J. Chem. Thermodyn.* **1978**, 10, 483.
- (22) Engels, P.; Schneider, G. M. *Ber. Bunsen-Ges. Phys. Chem.* **1972**, 76, 1239.
- (23) Marczak, W.; Ernst, S. *Bull. Pol. Acad. Sci. Chem.* **1998**, 46, 375. Marczak, W. *J. Chem. Eng. Data* **1996**, 41, 1462.
- (24) Marczak, W.; Giera, E. *J. Chem. Thermodyn.* **1998**, 30, 241.
- (25) Najdanovic-Visak, V.; Esperança, J. M. S. S.; Rebelo, L. P. N.; Nunes da Ponte, M.; Guedes, H. J. R.; Seddon, K. R.; Szydlowski, J. *Phys. Chem. Chem. Phys.* **2002**, 4, 1701.
- (26) de Sousa, H. C.; Rebelo, L. P. N. *J. Polym. Sci. B: Polym. Phys.* **2000**, 38, 632.
- (27) Schneider, G. *Ber. Bunsen-Ges. Phys. Chem.* **1966**, 70, 497.
- (28) It should be noted that, in turn, φ_i can be approximated to a weight fraction since the ratio between the molecular weights of 3-MP and (H/D) water shifts from 5.2 to 4.7 upon deuteration on the solvent.
- (29) Kamide, K. *Thermodynamics of Polymer Solutions*; Elsevier: Amsterdam, 1990; Chapter 1. Rätzsch, M. T.; Kehlen, H. *Prog. Polym. Sci.* **1989**, 14, 1. Luszczek, M.; Van Hook, W. A. *Macromolecules* **1996**, 29, 6612. Enders, S.; de Loos, T. W. *Fluid Phase Equilib.* **1997**, 139, 335.
- (30) The word "basic" refers to phase diagrams with a single critical concentration and a maximum of two corresponding critical points in the $T-x$ or $p-x$ projections.
- (31) Rebelo, L. P. N.; Visak, Z. P.; de Sousa, H. C.; Jancsó, G.; Lopes, J. C.; Szydlowski, J. Manuscript in preparation.
- (32) Prigogine I.; Defay, R. *Chemical Thermodynamics*; Everett, D. H., translator; Longmans Green & Co.: London, 1954; pp 271–290.
- (33) Rebelo, L. P. N.; Najdanovic-Visak, V.; Visak, Z. P.; Nunes da Ponte, M.; Troncoso, J.; Cerdeiría, C. A.; Romani, L. *Phys. Chem. Chem. Phys.* **2002**, 4, 2251.
- (34) Brovchenko, I. V.; Oleinikova, A. V. *J. Chem. Phys.* **1997**, 106, 7756 and references therein.
- (35) Papai, I.; Jancsó, G. *J. Phys. Chem. A* **2000**, 104, 2132 and references therein.
- (36) Almásy, L.; Cser, L.; Jancsó, G. *J. Mol. Liq.* **2002**, 101, 89.
- (37) Narayanan, T.; Prafulla, B. V.; Kumar, A.; Gopal, E. S. R. *Ber. Bunsen-Ges. Phys. Chem.* **1991**, 95, 12.